Published in final edited form as:
J Neurosci. 2013 January 9; 33(2): 761–775. doi:10.1523/JNEUROSCI.3896-12.2013.

Postsynaptic ERG potassium channels limit muscle excitability to allow distinct egg-laying behavior states in *C. elegans*

Kevin M. Collins and **Michael R. Koelle***
Department of Molecular Biophysics and Biochemistry, Yale University, New Haven, CT USA

Abstract

C. elegans regulates egg laying by alternating between an inactive phase and a serotonin-triggered active phase. We found that the conserved ERG potassium channel UNC-103 enables this two-state behavior by limiting excitability of the egg-laying muscles. Using both high-speed video recording and calcium imaging of egg-laying muscles in behaving animals, we found that the muscles appear to be excited at a particular phase of each locomotor body bend. During the inactive phase, this rhythmic excitation infrequently evokes calcium transients or contraction of the egg-laying muscles. During the serotonin-triggered active phase, however, these muscles are more excitable and each body bend is accompanied by a calcium transient that drives twitching or full contraction of the egg-laying muscles. We found that ERG null mutants lay eggs too frequently, and that ERG function is necessary and sufficient in the egg-laying muscles to limit egg laying. ERG K^+ channels localize to postsynaptic sites in the egg-laying muscle, and mutants lacking ERG have more frequent calcium transients and contractions of the egg-laying muscles even during the inactive phase. Thus ERG channels set postsynaptic excitability at a threshold so that further adjustments of excitability by serotonin generate two distinct behavioral states.

Introduction

Changes in synaptic strength allow animals to enter different behavioral states and underlie various forms of learning and memory. Synaptic plasticity is regulated by mechanisms that function on different timescales, from seconds to years. Neurotransmitter signaling through G protein coupled receptors affects cell and synaptic excitability within seconds via regulation of plasma membrane and intracellular ion channels (McDonald et al., 1994). This kind of modulatory signaling alters neural circuit activity and behavior (Marder and Bucher, 2007). The resulting short-term changes in synaptic Ca^{2+} signaling regulate more stable forms of synaptic plasticity including long-term potentiation or long-term depression (Lüscher et al., 2000). Dissecting the molecular basis of synaptic excitability and how it is regulated by fast and slow plasticity is critical to understanding behavior. Because most studies focus on synaptic connections within complex neural circuits, the precise relationships between molecules, synaptic excitability, and behavioral output *in vivo* remain poorly understood.

C. elegans egg-laying behavior offers many experimental advantages for studying the molecular basis of synaptic activity and its modulation during distinct behavior states. Egg laying is controlled by a simple circuit in which eight motor neurons, which themselves receive little synaptic input, form a large synapse onto a set of vulval muscles and stimulate

*To whom correspondence should be addressed (michael.koelle@yale.edu), Department of Molecular Biophysics and Biochemistry, Yale University School of Medicine, 333 Cedar Street, SHM CE30, P.O. Box 208024, New Haven, CT 06520-8024 USA, tel: (203) 737-5808; fax: (203) 785-6404.

The authors declare no competing financial interests.

their contraction. Egg laying involves alternating between two distinct behavioral states: quiescent periods of about 20 minutes during which no egg laying occurs and egg-laying active phases lasting several minutes. The active phases appear to result when two of the motor neurons release serotonin to act via G protein coupled receptors on the vulval muscles and increase their excitability (Waggoner et al., 1998; Hapiak et al., 2009). Strong regulation is superimposed on the pattern of alternating egg laying behavioral states. For example, worms virtually halt egg laying in the absence of food and rapidly restart the behavior when re-fed (Dong et al., 2000). Egg laying has been studied genetically for decades, and dozens of genes have been identified by mutations that either block (Desai et al., 1988) or increase egg laying (Bany et al., 2003). However, the activity of the underlying egg-laying motor circuit and how it is modulated by serotonin have not been well defined. The ability to leverage egg-laying mutants to understand the molecular mechanisms that regulate synaptic function has been limited by the tools available to analyze the egg-laying synapse and its behavioral output.

In this work, we developed new imaging and behavioral assays that allowed us to analyze the structure, activity, and behavioral output of the egg-laying synapse. We used these tools to determine how the ERG K^+ channel functions at the egg-laying synapse to allow serotonin to generate distinct active and inactive behavioral states for egg laying.

Materials and Methods

Nematode Culture, Strains, and Maintenance

Caenorhabditis elegans strains were maintained as hermaphrodites 20°C on Nematode Growth Medium (NGM) agar plates with *E. coli* OP50 as a source of food as described (Brenner, 1974). All strains are derived from the Bristol N2 wild-type strain, and all assays were performed using age-matched adult hermaphrodites 24–40 hours past the late L4 stage. *unc-103* alleles were isolated via EMS mutagenesis (Bany et al., 2003; Bellemer et al., 2011): *vs39* (C507Y), *vs157* (S607fs), *vs158* (S302F).

Molecular Biology and Transgenes

Transgenes were generated by microinjection of plasmid DNA into hermaphrodites. For expression of wild-type ERG in all vulval and body wall muscles, a cDNA for the vulval muscle-expressed isoform, *unc-103e* (Reiner et al., 2006), was inserted into pPD96.52 (1999 Fire Lab Vector kit) between the *myo-3* promoter and *unc-54* 3′ untranslated region (UTR) to generate plasmid pKMC134. This plasmid, or the empty vector control, were co-injected with a plasmid expressing GFP in muscle (pAB25, Bellemer et al., 2011) at 5ng/μl each along with the *lin-15* rescuing plasmid pL15EK (Clark et al., 1994) (50ng/μl) into LX1476 *unc-103(sy673, e1597dm); lin-15(n765ts)* animals. For re-expression in the HSN, coding sequences for the HSN-expressed ERG isoform, *unc-103f* (Garcia and Sternberg, 2003; Reiner et al., 2006), were inserted into the empty vector pJM66A (Moresco and Koelle, 2004) between the *tph-1* promoter and *unc-54* 3′ UTR to generate pKMC112. To help increase expression levels to ensure that any failure to observe phenotypic rescue was not due to weak expression form the *tph-1* promoter, introns 5–10 were retained in the *unc-103f* coding sequence (see below). Similar results were seen with the *unc-103f* cDNA bearing no introns (data not shown). pKMC112 (ERG) or the corresponding empty vector (pJM66A) were co-injected with a plasmid expressing GFP in the HSN (pJM60A, (Moresco and Koelle, 2004) at 80ng/μl each along with the L15EK rescue plasmid (50ng/μl) into LX1476 animals. Egg-laying behavior was assayed in five independent lines per transgene.

Tissue-specific expression of dominant-negative ERG and EAG channels

The following two complementary oligonucleotides were used to mutate sequences encoding the GFG residues in the ERG K^+ selectivity filter to AAA by Quickchange mutagenesis: 5′-CA TTA TCC ACA ATT ACA TCT ATC GCG GCC GCT AAT GTA TCG GCG ACG ACA G-3′ and 5′-C TGT CGT CGC CGA TAC ATT AGC GGC CGC GAT AGA TGT AAT TGT GGA TAA TG-3′. For expression of dominant-negative ERG in muscles, pKMC134 was mutagenized to generate pKMC140 (DN-ERG). For expression in the HSN, pKMC112 was mutated to generate pKMC117 (HSN-DN-ERG). Correct mutagenesis was confirmed using the introduced *NotI* restriction site (underlined) and DNA sequencing. To generate a dominant-negative EAG, the *egl-2* cDNA was first amplified from pLR120 (LeBoeuf et al., 2007) and inserted into the muscle expression vector pPD96.52 to generate pKMC186. The following two complementary oligonucleotides were used to mutate sequences encoding the GFG residues in the EAG K^+ selectivity filter to AAA by Quickchange mutagenesis: 5′-ATG AGT TGT ATG TCG ACA GTT GCG GCC GCT AAC ATT GCT AGT AAT ACA GAC-3′ and 5′-G TCT GTA TTA CTA GCA ATG TTA GCG GCC GCA ACT GTC GAC ATA CAA CTC AT-3′. For expression of dominant-negative EAG in muscles, pKMC186 was mutated to generate pKMC214. As above, mutagenesis was confirmed using the introduced *NotI* restriction site (underlined) and DNA sequencing. For expression in muscles, pPD96.52 (empty vector control), pKMC140 (DN-ERG), or pKMC186 (DN-EAG) were injected at 2ng/μl with pAB25A (4ng/μl; expresses GFP in muscles) and the *lin-15* rescuing plasmid L15EK rescue plasmid (50ng/μl) into MT8189 *lin-15(n765ts)* animals. For expression in the HSN, pJM66A (empty vector control) or pKMC117 (HSN-DN-ERG) were injected with pJM60A (expresses GFP in HSN) at 80ng/μl each along with the L15EK rescue plasmid (50ng/μl) into MT8189 animals. Egg-laying behavior was assayed in five independent lines per transgene.

Vulval muscle-specific fluorescent reporter transgenes

A ~2.6 kB DNA fragment upstream of the *unc-103e* start site was amplified from genomic DNA by PCR with the following oligonucleotides: 5′-GGA ACTAGT GCATGC CTA TTT TAT ATT TAC AAT ATT TTA G-3′ and 5′-TCA GCG CCCGGG ACC ACC ACC ACC ACA ACC-3′. This DNA fragment was ligated into pPD49.26 bearing the *unc-54* 3′UTR (Mello and Fire, 1995) to generate pKMC189. Into this vector, coding sequences for GFP (Moresco and Koelle, 2004), GCaMP3 (Tian et al., 2009), mCherry (McNally et al., 2006), or mCD8 (Lee and Luo, 1999) fused to mCherry were inserted to generate pKMC188, pKMC265, pKMC257, and pKMC191, respectively. To generate the vulval muscle TM-mCherry reporter, pKMC191 (mCD8-mCherry, 5ng/μl) was injected along with the L15EK rescue plasmid (50ng/μl) into MT8189 animals. The reporter transgene was integrated into chromosomes using UV/Trimethylpsoralen, and four independent integrants (*vsIs146 to vsIs149*) were recovered and backcrossed to the wild type six times. Other than expression level, there were no apparent differences among the integrants in the pattern of TM-mCherry expression. For double labeling of the vulval muscles with the HSN and VC motor neurons, LX1693 animals carrying *vsIs147* were crossed with LX693 animals carrying the *vsIs44* transgene, which expresses GFP from the *tph-1* promoter (Tanis et al., 2008) to generate LX1847 animals. For double labeling of the vulval muscles with the VC presynaptic terminus, LX1695 animals carrying *vsIs149* were crossed with TV7979 animals carrying the *wyIs222* transgene (Spilker et al., 2012) which expresses GFP::RAB-3 from the *unc-4* promoter to generate LX1865 animals. To construct the vulval muscle calcium reporter, pKMC265 (GCaMP3, 20ng/μl) and pKMC257 (mCherry, 2ng/μl) were injected along with the L15EK rescue plasmid (50ng/μl) into MT8189 animals. The GCaMP3 reporter transgene was integrated as above, and four independent integrants (*vsIs150 to vsIs153*) were recovered and backcrossed to the wild type six times. There were no detectable differences in expression pattern among the integrants. LX1776 carrying the *vsIs153*

transgene had the lowest level of expression and no apparent phenotypic abnormalities. To reduce blue-light sensitivity during imaging, KG1180 animals carrying the *lite-1(ce314)* mutation (Edwards et al., 2008) were crossed to LX1776 animals to generate LX1848 *vsIs153; lite-1(ce314)* animals. To move the *vsIs153* reporter into the ERG W85stop null mutant background, LX1442 animals were mated with KG1180 animals and the cross progeny were crossed with LX1848 animals to generate LX1849 *vsIs153; unc-103(sy673, e1597dm); lite-1(ce314)* animals. A control transgene *(vsEx733)* expressing GFP and mCherry in the vulval muscles from the *unc-103e* promoter was prepared by injecting pKMC188 (GFP, 2ng/μl) and pKMC257 (mCherry, 2ng/μl) along with L15EK rescue plasmid into LX1832 *lite-1(ce314), lin-15(n765ts)* animals to generate LX1901.

Single-copy MosSCI transgenes

The *unc-103* 3′ UTR region was amplified from genomic DNA by PCR using the following oligonucleotides: 5′-TGA CTCGAG GGTACC ACGCGT CCC GGT TTC TCT CTT TCT CTG-3′ and 5′-CGC CTTAAG GCC TTT TTG CAC TGT TGA GTG-3′. The amplified 3′UTR and the vulval muscle-specific *unc-103e* promoter (above) were inserted into pCFJ151 (Frøkjaer-Jensen et al., 2008) to generate the empty vulval muscle-specific MosSCI vector pKMC176. To ensure robust ERG::GFP expression from single copy transgenes, an *unc-103e* genomic cDNA/genomic DNA hybrid was first constructed in pUC19. Briefly, *unc-103* exons 5 to 11 were PCR-amplified from worm genomic DNA and inserted into the *unc-103e* cDNA at unique *BstXI* and *AccI* sites to generate pKMC100. To make a functional ERG-GFP fusion, a *NotI* site was inserted into pKMC100 near the 3′ end of *unc-103e* in a region encoding five consecutive glycine residues by Quickchange mutagenesis using the following complementary oligonucleotides to generate pKMC178: 5′-CGT CTT CCG AAT GGA GGT GGT GCG GCC GCT GGA GGT GGT GTT GTC GAT GAG ATG AGA GTC-3′ and 5′-GAC TCT CAT CTC ATC GAC AAC ACC ACC TCC AGC GGC CGC ACC ACC TCC ATT CGG AAG ACG-3′. Coding sequences for GFP were then inserted at the *NotI* site in pKMC178 to generate pKMC179. Wild-type *ERG::GFP* was amplified from pKMC179 by PCR and inserted into the MoSCI vector pKMC176 to generate pKMC180. Coding sequences for the ERG C-terminal PDZ interaction motif (-DTIL) were replaced by a stop codon (ERG::GFPΔPDZ) to generate pKMC204. To isolate *C. elegans* strains carrying single-copy ERG-GFP inserts, the MosSCI plasmids pKMC180 or pKMC204 (50ng/μl) were injected into EG4322 animals bearing the *ttTi5605 Mos1* transposon as described (Frøkjaer-Jensen et al., 2008). Correct replacement of the *Mos1* transposon by the single-copy transgene (*vsSi1*, wild-type ERG::GFP; *vsSi11*, ERG::GFPΔPDZ) was confirmed by DNA sequencing and expression of GFP. To check for phenotypic rescue, animals bearing *vsSi1* or *vsSi11* transgenes were crossed with LX1442 ERG null mutants (W85Stop) to generate strains LX1678 and LX1685, respectively. For double labeling of MosSCI transgenes with the vulval muscle TM-mCherry reporter, *vsIs149* was crossed into LX1678 and LX1685 animals.

Behavior Assays and Video Recording

Unlaid eggs and early-stage egg laid eggs were quantitated as described using age-matched adult hermaphrodites 24–40 hours past the late L4 stage (Chase and Koelle, 2004). For bright-field recording of behaving animals, a Casio EX-FC150 camera was mounted onto an eye tube of a Zeiss Axiovert 100 using Unilink and Linkarm adaptors (Brunel Microscopes Ltd.). Animals were followed by manually moving a gliding stage. To measure intervals between egg-laying events (Figure 5), single hermaphrodite animals were picked to NGM plates seeded with 30μl of an OP50 bacterial culture. Video recordings were carried out through a 10x objective at 30 frames per second (fps) at 640×480p. Videos were analyzed for timing of egg-laying events and distance to adjacent smooth contractions and relaxations using ImageJ. To measure vulval muscle twitching behavior and Ca^{2+} transients in behaving

animals, a small amount of OP50 bacteria was scooped onto a platinum wire and used to pick one worm to an unseeded NGM plate. A ~20×20mm chunk was immediately taken from the plate and placed worms-side down onto a 24×60mm #1 coverslip and overlaid with a 22×22mm #1 coverslip. The worms were allowed to recover for 1–2 hours in a humidified chamber at 20°C, by which time egg-laying behavior was observed to be similar to that observed in unmounted animals. Bright-field videos were recorded through a 40x Nomarski objective at 120Hz at 640×480p. Timing of smooth contractions, relaxations, twitches, and egg-laying events were recorded from videos using Etho Timer (Liu and Thomas, 1994). Statistical analyses for all data were performed using JMP version 9.0 (SAS Institute) or Prism 9.0, and error bars indicate 95% confidence intervals.

Confocal Microscopy and Ratiometric Imaging

To visualize the egg-laying system and sub-cellular localization of ERG, age-matched adult hermaphrodite worms expressing fluorescent reporter transgenes were immobilized using 10mM muscimol on 3% agarose pads and covered with #1 coverslips. Two-channel confocal Z-stacks with a pinhole size of 1 Airy unit (0.9 μm thick optical sections, 12-bit images) were obtained with a Zeiss 710 Duo confocal microscope with a 63x Water C-Apochromat objective (1.2NA) using the LSM head. For Ca^{2+} imaging in behaving animals, single two-channel confocal slices (18 μm thick) were collected through a 20x Plan-Apochromat objective (0.8NA) using the 710 Duo LIVE head. Short-term (one minute) recordings were collected at 30 fps at 512×512 pixel, 12-bit resolution while longer-term (6 minute) recordings were collected at 20 fps at 256×256 pixel, 16-bit resolution. The stage and focus were adjusted manually to keep the egg-laying system in view and focused during recording periods. Ratiometric analysis for both Z-stacks and Ca^{2+} recordings was performed in Volocity (version 5, Perkin Elmer). Briefly, separate ratio and intensity-modulated ratio channels were calculated from GCaMP3 (or GFP) and mCherry fluorescence channels. Voxels with mCherry fluorescence intensities 2 standard deviations above background were selected as objects for measurement. Intensity-modulated images show false colors representing the GCaMP3/mCherry or GFP/mCherry ratio displayed at the brightness of the corresponding mCherry voxels. Ca^{2+} transients were identified by visual inspection of ratio traces. For 1-minute recordings, the prior local minimum in GCaMP3/mCherry ratio was used to establish a baseline for $\Delta R/R$ determination. For 6-minute recordings, the data were first smoothened using a 150 msec (three timepoint) rolling average, and the lowest 10% of the GCaMP3/mCherry ratio values were averaged to establish a $\Delta R/R$ baseline. To study synapse-specific features in Z-stacks (Figure 4), a 12μm (x) × 10μm (y) × 6μm (z) box was manually placed on the synaptic region and measurements of fluorescence within this synaptic region were obtained as described above.

Results

Anatomy of the egg-laying synapse

We developed tools to visualize the egg-laying system. Eight vulval muscle (vm) cells, four each of the vm1 and vm2 class, contract to open the vulva and release eggs, and two types of motor neurons synapse onto these muscles (Figure 1) (White, J.G. et al., 1986). The Ventral C (VC) motor neurons release acetylcholine (ACh) (Duerr et al., 2001) which activates nicotinic ACh receptors (nAChR) expressed on the vulval muscles to drive contraction and egg laying (Waggoner et al., 2000; Kim et al., 2001). The Hermaphrodite Specific Neurons (HSN) are motor neurons that release serotonin to put the vulval muscles in a more excitable state (Weinshenker et al., 1995; Shyn et al., 2003). To visualize both sides of the egg-laying synapses, we expressed a membrane-localized mCherry protein in all eight vulval muscles to label the surface of these cells, and simultaneously expressed GFP in the HSN and VC neurons (Figure 1B). We found that each vm2 cell extends a dendrite-like postsynaptic

process laterally that meets and apposes the HSN and VC presynaptic release sites (Figure 1B, arrowheads and inset boxes). Synaptic contacts form over about 10 μm on both the left and right sides of the animal in what may be the largest synapses in *C. elegans*. By expressing the presynaptic marker GFP::RAB-3 in all cholinergic neurons (Figure 1C), we again saw the large lateral synapses that VC4 and VC5 make onto the vm2 cells. We also observed additional cholinergic presynaptic termini close to the vm2 muscle arms that extend along the right ventral cord. Most of these are likely to be VC synapses onto the vm2 cells, but a few may represent the synapses of the VA7, VB6, and VD7 ventral cord motor neurons onto the vm1 muscles (White, J.G. et al., 1986).

The ERG K^+ channel inhibits *C. elegans* egg-laying muscle activity

We screened for *C. elegans* mutants with increased egg-laying behavior, which could result from increased presynaptic excitation or from increased postsynaptic excitability of the vulval muscles. In our first screen, we isolated mutants that lay their eggs prematurely (Bany et al., 2003). The embryos from these mutants are laid shortly after fertilization, when they are still at early stages of development. We separately screened for mutations that suppress a block in neurotransmitter release from HSN caused by an *egl-47(dm)* mutation (Tanis et al., 2009). One mutation from the first screen and two mutations from the second screen all mapped to the location of the *unc-103* gene and failed to complement each other as well as an *unc-103* null mutation. Sequencing revealed that each mutant had a single base-pair lesion in the *unc-103* gene.

unc-103 is the sole *C. elegans* ortholog of ERG (Ether-a-go-go (EAG) Related Gene), which encodes a conserved, voltage-gated K^+ channel that inhibits cell excitability (Garcia and Sternberg, 2003; Reiner et al., 2006). As shown in Figure 2A, ERG channels have six transmembrane domains, including a voltage sensor, and a cytoplasmic cyclic nucleotide binding domain (cNBD). *C. elegans* ERG is ~70% identical to the human ERG (hERG) in the transmembrane segments and cNBD. Although *C. elegans* ERG lacks the N-terminal PAS domain found in other ERG and EAG channels, it bears a PDZ-interaction motif at its C-terminus that may bind other proteins to mediate subcellular localization. *unc-103* was originally identified by a gain-of-function mutation in the sixth transmembrane domain (A331T) which causes uncoordinated locomotion and a block in egg laying (Figure 2C). hERG channels bearing this mutation (A653T) open more readily upon membrane depolarization (Petersen et al., 2004). Thus, the A331T gain-of-function mutation likely increases ERG K^+ channel activity and thereby inhibits the electrical excitability of cells that express it. Our three newly-identified ERG mutations (Figure 2A) were phenotypically similar to two previously known *unc-103* null mutants in showing well-coordinated locomotion but increased egg laying, as evidenced by retaining fewer unlaid eggs (Figures 2D and 2E), and laying eggs at early stages of development (data not shown). These and other previously reported results (Reiner et al., 2006) show that the ERG K^+ channel normally inhibits *C. elegans* egg-laying behavior.

C. elegans ERG may act to oppose membrane depolarization mediated by L-type Ca^{2+} channels. In the human heart, hERG acts to repolarize the heart muscle during long ventricular action potentials mediated by L-type Ca^{2+} channels (Sanguinetti and Tristani-Firouzi, 2006). In *C. elegans*, L-type Ca^{2+} channels mediate action potentials and are encoded by the *egl-19* gene (Gao and Zhen, 2011; Liu et al., 2011). Gain-of-function *egl-19(gf)* mutations increase Ca^{2+} channel activity, causing excessive muscle excitability and hyperactive egg laying (Lee et al., 1997). The *egl-19(gf)* hyperactive egg-laying phenotype was similar to that of ERG null mutants (Figure 2E, compare bars 8 and 9). Conversely, an *egl-19(lf)* mutant with decreased Ca^{2+} channel activity accumulated unlaid eggs, similar to animals bearing the A331T gain-of-function ERG mutation (Figure 2E, compare bars 10 and 2). We found that combining loss-of-function mutations for ERG and

EGL-19 that individually caused opposite egg-laying defects led to an intermediate phenotype close to that of the wild type (Figure 2E, bar 11). The reduction in unlaid eggs in the *unc-103(W85stop), egl-19(lf)* double mutant was not caused by a defect in egg production, as average brood sizes in the single and double mutants were not statistically different (*egl-19(lf)*, 197±12; *unc-103 (W85stop)*, 196±30; *unc-103 (W85stop), egl-19(lf)*, 165.3±39). These results suggest that *C. elegans* ERG, like hERG in human heart muscle, antagonizes excitation caused by L-type Ca^{2+} channels.

We next determined in which cells ERG acts to inhibit egg-laying behavior. The HSN motor neurons release serotonin and promote the induction of the active phase of egg-laying behavior. Animals lacking the HSNs are egg-laying defective, accumulating 50 unlaid eggs (Figure 3A). This strong egg-laying defect of HSN(−) animals was partially suppressed in ERG null mutants, but the animals remained egg-laying defective, accumulating ~25 eggs, significantly more than the wild type (Figure 3A). This result shows that ERG acts at least in part outside the HSN to promote egg laying, but that ERG null mutants also require HSN function to show hyperactive egg-laying.

Previous work has shown that six distinct promoters (a–f) drive expression of ERG isoforms with different N-termini in all muscle cells and many neurons, including the vulval muscles and HSN (Garcia and Sternberg, 2003; Reiner et al., 2006). We found that re-expression of the vulval muscle expressed ‘e’ isoform of ERG in vulval muscle using the muscle-specific *myo-3* promoter fully rescued the hyperactive egg-laying defect of ERG null mutants (Figure 3B, compare bars 4 to 5). Re-expression of the HSN expressed ‘f’ isoform of ERG in HSN using the *tph-1* promoter was unable to rescue (Figure 3B, bars 6 and 7). These results indicate that ERG function in muscle is sufficient to inhibit egg-laying behavior.

To test where ERG function was necessary, we analyzed egg-laying behavior in animals transgenically expressing a dominant-negative ERG mutant. We adapted a previously described dominant-negative mutant of the GIRK2 K^+ channel (Kuzhikandathil and Oxford, 2000) in which mutation of the GYG residues in the K^+ selectivity filter to three alanines (AAA) dominantly blocks activity of wild-type GIRK2 subunits that assemble into tetramers with the mutant (Figure 3C, left). We mutated the corresponding GFG in ERG to AAA and expressed this DN-ERG in wild-type animals from either the muscle- or HSN-specific promoters. Expression of DN-ERG in muscle caused hyperactive egg laying (Figure 3C, compare bars 4 and 5). This effect was specific to ERG, as expression of the analogous dominant-negative mutant of the related EAG channel EGL-2 had no effect (Figure 3C, bar 6), even though EGL-2 is also expressed in the vulval muscles (Weinshenker et al., 1999). Expression of DN-ERG in the HSN caused a significant reduction in the number of unlaid eggs, suggesting that ERG does regulate the electrical excitability of the HSN. However, this phenotype was weaker than that seen for muscle-specific inactivation of ERG.

Together, our results show that ERG acts in vulval muscles to inhibit egg-laying behavior, presumably by inhibiting the electrical excitability of these muscles. ERG has an additional, weaker effect inhibiting egg laying by acting in the HSN neurons.

ERG localizes to the vulval muscle postsynaptic termini via a PDZ interaction motif

We found that within vulval muscles, ERG is subcellularly enriched at postsynaptic termini. We transgenically expressed a fusion protein in which GFP was inserted into ERG just upstream of its C-terminal PDZ interaction motif. The *unc-103e* promoter (Reiner et al., 2006), was used in a single-copy, chromosomally-inserted transgene to achieve low-level expression specifically in the vulval muscles. We used a control transgene to express a red fluorescent protein, consisting of the murine CD8 protein fused to mCherry, which is passively distributed within the plasma membrane of the vulval muscles. Ratiometric

confocal fluorescence imaging showed that ERG::GFP was enriched at two locations within the vm2 that correspond to the two different postsynaptic sites in these muscles (Figure 4A). First, we saw enrichment at the ends of the lateral processes that serve as the postsynaptic termini onto which the HSN and VC neurons make synaptic contacts. Second, we saw localization along the muscle arms of the right vm2s onto which the right ventral cord neurons make synapses. In addition to being enriched at the postsynaptic termini, ERG::GFP was also found at lower levels uniformly over the vulval muscle plasma membrane. Quantifying the ERG::GFP to membrane mCherry ratio in voxels from a subregion containing the vm2 lateral processes of multiple animals showed that ERG::GFP is significantly enriched at the lateral postsynaptic region compared to its levels averaging voxels over the entire vulval muscle (Figure 4C, compare 1 and 2).

To test whether the synaptic enrichment of ERG was mediated by its C-terminal PDZ-interaction motif, we generated another single-copy transgene that expressed an ERG::GFPΔPDZ mutant in which the last four residues (DTIL) were deleted. This mutant protein lacked the synaptic enrichment seen for wild-type ERG::GFP (Figure 4B). Indeed, ERG::GFPΔPDZ was actually depleted from the postsynaptic terminus (Figure 4C, compare 3 and 4). This was not due to a change in expression levels, as the ratio of GFP to mCherry over the entire vulval muscle was identical in the strains expressing wild-type ERG::GFP versus ERG::GFPΔPDZ (Figure 4C, compare 1 and 3). These results show that ERG localizes in vulval muscle to postsynaptic termini via a PDZ interaction motif, presumably by binding an unidentified PDZ domain-containing protein localized to synapses.

To test whether ERG localization to the synapse is important for its function, we compared the ability of wild-type and ΔPDZ ERG::GFP single-copy transgenes to rescue the hyperactive egg laying defect of ERG null mutants. Re-expression of wild-type ERG::GFP partially rescued the number of unlaid eggs toward wild-type levels, while the ERG::GFPΔPDZ mutant produced less rescue in this assay (Figure 4D, top, compare bars 3 and 4). These data are compromised by the fact that ERG null mutants fail to accumulate eggs both due to hyperactive egg laying and due to a failure to produce a normal number of eggs; the latter defect cannot be rescued by re-expression of ERG just in the vulval muscles. Thus we used a second assay of egg-laying behavior less sensitive to defects in egg production in which we measured the developmental stage of freshly-laid eggs (Chase and Koelle, 2004). While wild-type animals laid about 10% of their eggs at early stages of development, ERG null mutants laid more than 80% of their eggs at early stages (Figure 4D, bottom, compare bars 5 and 6). Re-expression of wild-type ERG::GFP in the vulval muscles completely rescued this measure of hyperactivity, while the ERG::GFPΔPDZ mutant was unable to fully rescue. Previous work has identified an ERG isoform generated by alternative splicing that leads to the premature termination of the protein upstream of the PDZ interaction motif (Reiner et al., 2006). This suggests that some native ERG channels may be functional outside of PDZ complexes, and indeed we see significant rescue when ERG::GFPΔPDZ mutant is the sole ERG expressed in the vulval muscles (Figure 4D). However, our results show that the ERG ‘e’ isoform expressed in vulval muscle is enriched at the postsynaptic terminus via its PDZ interaction motif and that this localization is required for proper inhibition of egg-laying behavior.

Vulval muscle contractions are phased with respect to body bends and inhibited by ERG

To understand more precisely how ERG affects egg-laying behavior, we video recorded and quantitatively analyzed this behavior in wild-type and ERG null mutant animals as they moved freely on the standard NGM agar plates used for *C. elegans* growth in the lab. As seen previously (Waggoner et al., 1998), wild-type animals enter an active phase for several minutes during which a cluster of eggs is laid, followed by an inter-cluster interval with no egg laying that lasts about 20 minutes until the start of the next active phase (Figure 5A and

5B). ERG null mutants usually laid single eggs rather than clusters of eggs, probably in part because the adults have only ~two eggs in their uterus of which only one may be in position to be laid (Figure 5B). However, ~25% of egg laying events in the ERG null mutant were in clusters of two or more eggs (Figure 5B and data not shown), indicating the ERG null mutant does have active phases for egg laying. Loss of ERG reduced the interval between egg-laying events. In wild-type animals, this interval averaged 17.5±1.2 minutes, while in ERG null mutants it was reduced to 11.2 ±0.3 minutes (Figure 5B). This direct observation of the increased egg laying by the ERG null mutant accounts for the phenotypes observed in less direct assays of egg-laying behavior (Figures 2E).

We noticed in our videos that eggs were often laid during locomotion when the vulva was at a particular phase of a body bend. *C. elegans* moves with sinusoidal body bends consisting of waves of body wall muscle contraction and relaxation driven by ventral nerve cord motor neurons. ACh drives contraction while GABA causes relaxation (Figure 5C, top). We subdivided an idealized waveform into six parts and determined which subdivision contained the vulva at the time each egg was laid. We found that egg laying increased in frequency as the vulva neared a ventral contraction and was subsequently inhibited until after the vulva passed through this contraction (Figure 5C). We saw a similar trend for ERG null mutants (data not shown).

For a higher-resolution analysis, we developed conditions to directly observe vulval muscle contractions in behaving animals. The experiments shown in Figure 5, like almost all previous studies of *C. elegans* egg-laying behavior, infer the occurrence of vulval muscle contractions indirectly and only when they result in an egg being laid. Using a relatively high-magnification (40X) objective lens, video recording at 120 frames per second to capture rapid contractions, and continuously moving the microscope stage to keep the vulva in the field of view, we could directly view vulval muscle contractions as worms moved. We found that in both the wild type and in ERG null mutants, the vulval muscles undergo three distinct types of contraction (Figure 6A and Movie 1). First, we observed slow, smooth contractions and relaxations during every body bend similar to those of the adjacent body wall muscles. The slow, smooth vulval movements might be due to active contraction of the vulval muscles themselves, or might simply result from passive compression and stretching of the vulval region as the adjacent body wall muscles contract and relax during body bends. Second, we observed more rapid contractions, which we refer to as twitches, that visibly moved the vulva, and that often occurred independently on either the anterior or posterior side of the vulva (Figure 6A). Finally, a third type of contraction, stronger than a twitch and always occurring on both anterior and posterior sides of the vulva, was used to release eggs. In the wild type, smooth contraction at the vulva occurred during every body bend (Movie 1), but as detailed below, twitches and egg-laying contractions occurred about 15% and 5% as frequently, respectively.

We found that twitches, like egg-laying events, were phased with respect to body bends. Because the narrow field of view of our high-magnification videos did not allow us to see an entire body bend waveform, we determined the timing of the twitch relative to the smooth contractions and relaxations at the vulva (Figure 6B). We found that twitching dramatically increased in frequency as the vulva neared a smooth contraction, and that twitching was subsequently inhibited until after a smooth relaxation (Figure 6B). This phasing of twitching with locomotion was reminiscent of but stronger than the phasing observed for egg laying, and was unchanged in ERG null mutants.

Strikingly, ERG null mutants had three times as many vulval twitches as did the wild type, with nearly half of all smooth contractions in the ERG null preceded by a twitch compared to only 15% in the wild type. (Figure 6C). We further analyzed whether twitch frequency

changed during the active periods of egg laying. In wild-type animals, vulval twitches became 2–3 fold more frequent during the active phase of egg laying, defined as a four minute period surrounding an egg-laying event (Figure 6C), and then declined back to a low level. In ERG null mutants, vulval twitching also increased during active periods of egg laying and then declined afterwards.

Together, these results suggest the hypothesis that the vulval muscles, like adjacent body wall muscles, receive an excitatory signal at a particular phase of every body bend. This rhythmic excitation sometimes results in a twitch or, more rarely, an egg-laying contraction, and the probability of a twitching or egg-laying response becomes higher during the active phase of egg laying. Our results show that ERG acts both during and between active phases to lower the probability that the rhythmic excitation leads to twitching or egg-laying responses.

Distinct, rhythmic Ca^{2+} transients in vulval muscles underlie twitches and egg-laying contractions

To more directly examine excitation of vulval muscles during locomotion, twitching, and egg laying, we co-expressed the Ca^{2+}-sensitive green fluorescent protein GCaMP3 (Tian et al., 2009) and the Ca^{2+}-insensitive red fluorescent protein mCherry in the vulval muscles and performed confocal imaging of behaving animals (Figures 7A–E, Movies 2 and 3). We found we could track the smooth contractions and relaxations of the vulval muscles during locomotion as changes in the area of mCherry fluorescence (Figures 7A, 7B, and 7F). By calculating the ratio of GCaMP3/mCherry fluorescence we could detect Ca^{2+} transients while correcting for changes in its fluorescence intensity caused by changes vulval muscle size, variations in focus, and movement (Figure 7F).

During the egg-laying active phase, we detected large Ca^{2+} transients in the vulval muscles accompanying most body bends (Figure 7F, right) as predicted from our analysis of egg-laying muscle contractions. Such fluorescence ratio changes were not observed in animals expressing the Ca^{2+}-insensitive GFP, even when they executed strong egg-laying contractions (Figure 7G), indicating that our recordings detect genuine Ca^{2+} transients and that effects of movement were removed by the ratiometric analysis used. During the egg-laying inactive phase, body bends typically lacked Ca^{2+} transients (Figure 7F, left), further demonstrating that the GCaMP/mCherry ratio transients we observed were not simply a consequence of animal movement or changes in vulval muscle size.

Just as egg-laying events (Figure 5C) and vulval muscle twitches (Figure 6B) are phased with respect to locomotor body bends, vulval muscle Ca^{2+} transients also showed similar phasing (Figure 7H), arguing that all result from the same rhythmic excitation of the egg-laying muscles that appears to occur at a particular phase of each body bend.

We plotted the peak amplitudes of all the Ca^{2+} transients in our recordings (Figure 7I) and found that they clustered into two distinct groups that we named twitch and egg-laying transients. In wild-type animals, the average change in GCaMP3/mCherry ratio ($\Delta R/R$) was ~50% for twitch transients, and 200% for egg laying transients.

Twitch Ca^{2+} transients (Figures 7C and 7D) appeared to underlie the twitching contractions observed during our bright-field movies of vulval muscle contractions. Like twitching contractions, twitch Ca^{2+} transients sometimes occurred on only the anterior or posterior side of the vulva (Figures 7C; Movies 2 and 3). Twitch Ca^{2+} transients also increased in frequency during egg-laying active phases (Figure 7F). Furthermore, twitching contractions were sometimes visible in the fluorescence recordings during twitch transients (Movie 3), despite the fact that the imaging conditions used were not well-suited to capturing such

movements. Egg-laying Ca^{2+} transients (Figure 7E, Movie 3) occurred simultaneously in both anterior and posterior vulval muscles, and were accompanied by the complete vulval openings that occur only during egg laying.

Twitch transients showed their peak magnitude at the ventral tips of the vulva (Figure 7C and 7D, arrowheads; Movies 2 and 3), a location distinct from the synaptic sites of the vulval muscles (Figure 1). Egg-laying transients also initiated at the ventral tips of the vulva but then spread throughout the vulval muscles (Movie 3). These results suggest that the twitch and egg-laying Ca^{2+} transients observed do not mainly result from local Ca^{2+} influx at synapses, but result from the propagation of excitation to distal sites in the vulval muscles. We did not detect any statistically significant difference in the amplitude of vulval muscle Ca^{2+} transients upon loss of ERG (Figure 7I). Thus while ERG channels appear to determine how sensitively the vulval muscle respond to the rhythmic excitation that occurs during each body bend, once release of Ca^{2+} is triggered, ERG has no further effect. The synaptic enrichment of ERG (Figure 4) is consistent with the idea that ERG specifically affects the initial excitation of the muscles at the egg-laying synapse.

ERG mutants have more frequent vulval muscle Ca^{2+} transients

To more fully capture changes in Ca^{2+} transient frequency during inactive and active egg-laying periods, we captured longer (6 min) recordings by adjusting our recording conditions to a slightly reduced temporal and spatial resolution. Twitch transients were sparse during the egg-laying inactive phase in wild-type animals (Figure 8A), precisely as we found through our bright-field recordings of vulval muscle twitching (Figure 6C). Ca^{2+} transients became much more frequent as animals entered an egg-laying active phase and then decayed back to a low level (Figure 8B). ERG null mutants also showed active phases with an increased frequency of Ca^{2+} transients (Figure 8D). However, ERG null mutants had more frequent Ca^{2+} transients even during the inactive phase (Figure 8C). We analyzed the duration of inter-transient intervals. Wild-type animals spent ~51% of our recordings in inactive periods with one Ca^{2+} transient or less per minute, while in ERG null mutants, this inactive period was reduced to ~36% of time spent (Figure 8E). Conversely, wild-type animals spent 25% of our recordings in more active periods with Ca^{2+} transients occurring every 20 seconds or less, while in ERG null mutants these active periods increased to 32% of time spent (Figure 8E). This increase in Ca^{2+} transient frequency in the ERG null mutant is consistent with our behavioral results showing that ERG null animals have more frequent egg-laying active phases and more frequent twitching contractions.

Together, our data indicate that in ERG null mutants, the primary defect that leads to hyperactive egg-laying behavior appears to be increased postsynaptic excitability, such that rhythmic synaptic stimulation of vulval muscles during each body bend produces responses closer to the threshold required to trigger Ca^{2+} transients. This leads to more frequent vulval muscle twitches and more frequent egg-laying contractions.

Discussion

We integrated molecular genetics, assays of subcellular localization, and both bright-field and fluorescent Ca^{2+}-indicator imaging of behaving animals to delineate how *C. elegans* sets excitability of the vulval muscles at the precise levels to allow egg-laying behavior to alternate between inactive and active states. Figure 9A schematizes key features of our results. Rhythmic excitation of vulval muscles at a particular phase of each body bend depolarizes the muscles. Between egg-laying active phases, subthreshold responses too weak to trigger detectable Ca^{2+} signaling or muscle contraction typically occur. During the serotonin-triggered egg-laying active phase, however, the muscles become more excitable so that rhythmic excitation triggers Ca^{2+} responses that drive twitching and egg-laying

contractions (Figure 9A). Loss of postsynaptic ERG K^+ channels elevates postsynaptic excitability both between and during egg-laying active phases, increasing the probability of postsynaptic Ca^{2+} transients that drive twitching and egg-laying contractions. Thus the two-state behavior seen in the wild type is degraded to a more continuous pattern of egg-laying muscle activity in ERG null mutants.

Figure 9B models at the cellular and molecular level how activity at the egg-laying synapse is controlled. ACh release from ventral cord motor neurons at a particular phase of each body bend activates vulval muscle nAChR to depolarize the vulval muscle postsynaptic terminus (Waggoner et al., 2000; Kim et al., 2001), accounting for the observed rhythmic excitation of the muscles. Depolarization activates the EGL-19 L-type Ca^{2+} channels to allow entry of Ca^{2+} through the plasma membrane and amplify the depolarization. *C. elegans* lacks voltage-gated Na^+ channels and thus uses only Ca^{2+} channels to generate action potentials (Gao and Zhen, 2011; Liu et al., 2011). ERG, in cooperation with other K^+ channels, repolarizes the membrane to antagonize the L-type Ca^{2+} channels to limit postsynaptic Ca^{2+} signaling so that, during the egg-laying inactive phase, no muscle contraction ensues. The active phase of egg-laying is produced by periodic serotonin release from the HSN (Waggoner et al., 1998; Shyn et al., 2003; Zhang et al., 2008). Serotonin activates two vulval muscle serotonin receptors that couple to the G proteins $G\alpha_q$ and $G\alpha_s$ (Carnell et al., 2005; Dempsey et al., 2005; Hobson et al., 2006). We observed large Ca^{2+} responses to the rhythmic excitations that occurred during the active phase. We propose that serotonin signaling initiates the egg-laying active phase by increasing postsynaptic electrical excitability beyond the threshold required to trigger Ca^{2+} transients and vulval muscle contraction (Figure 9B). To terminate egg laying an increase in postsynaptic inhibition, possibly driven by mechanosensation of egg release (Jose et al., 2007), reduces excitability of the vulval muscles. In our model, postsynaptic ERG channels adjust vulval muscle excitability so that during the inactive phase it lies just below the threshold needed to evoke Ca^{2+} transients and muscle contraction. Release of serotonin and possibly other modulatory factors can then determine when egg laying occurs. We anticipate that ERG functions similarly in neurons that express it to set excitability at thresholds that allow circuits and behaviors to achieve distinct inactive and active states.

Our analysis of postsynaptic excitability in the vulval muscles helps explain how regulation of neurotransmitter release from the presynaptic HSN can effectively control egg laying. Previous work has shown that $G\alpha_o$ and $G\alpha_q$ act in the HSN motor neurons to strongly regulate egg laying (Tanis et al., 2008). It is quite possible that much of the regulation of egg laying system, for example in response to sensory stimulation, occurs by controlling the timing and/extent of serotonin release from the HSN (Ringstad and Horvitz, 2008; Zhang et al., 2008).

Our work illuminates the results of previous studies of *C. elegans* egg-laying behavior. First, our observations of increased twitching and increased Ca^{2+} transients during the egg-laying active phase make concrete the existence of an active phase with increased vulval muscle excitability. This was previously hypothesized from the indirect evidence that egg-laying events are clustered in time (Waggoner et al., 1998) and the effects of exogenous serotonin on vulval muscle Ca^{2+} signaling (Shyn et al., 2003). Statistical analyses also suggested there was an underlying rhythmic pattern activating egg-laying events during the active phase, but the nature of the pattern generator remained unknown (Waggoner et al., 1998). Our work suggests that the pattern generator is or is coupled to the periodic body bends of locomotion. A previous study determined that serotonin released from the HSN stimulates a sharp increase in animal locomotion about 30 seconds prior to the onset of an active phase (Hardaker et al., 2001). The purpose for which the HSN simultaneously activates both body bends and the vulval muscles remained the object of speculation. Our work suggests that

locomotor body bends promote the rhythmic stimulation that triggers egg laying, and that it therefore makes sense for the worm to activate locomotion at the same time it turns up excitability of the vulval muscles to effectively generate egg-laying behavior.

How do body bends result in rhythmic excitation of the vulval muscles? One obvious potential source of rhythmic input to the vulval muscles is the ventral nerve cord motor neurons. The cholinergic VA and VB motor neurons that direct body wall muscle contraction during body bends also make synapses consisting of single active zones onto the vm1 vulval muscles (White, J.G. et al., 1986). However vulval muscle Ca^{2+} transients, twitches, and egg-laying events are initiated out of phase with contraction of the adjacent body wall muscles, arguing against the functional significance of these anatomically minor synapses. Far more extensive synapses onto the vulval muscles come from the six VC motor neurons. The VC neurons show rhythmic Ca^{2+} transients during locomotion (Faumont et al., 2011), but they only receive significant synaptic input from each other and the HSNs (White, J.G. et al., 1986). While VC4 and VC5 project short varicosities that synapse onto the vm2 lateral projections (Figure 1), VC1-3 and VC6 have long, anterior- and posterior-directed processes that synapse with each other along the body and with VC4/5 at the vulva (Bany et al., 2003). Twitches and egg laying typically start when VC1-3 enter the ventral contracted phase (see Figure 1A, bottom). We propose that the VC neurons provide postural, proprioceptive feedback to rhythmically excite the vulval muscles phased with body bends. In this role, the VCs would function like the DVA neuron, which extends processes along the ventral cord, mechanically senses body bends, and uses this information to modulate amplitude of the locomotion waveform (Li et al., 2006; Hu et al., 2011). The purpose of activating the vulval muscles in advance of ventral contraction is not clear, but it may mechanical. When the adjacent body wall muscles are relaxed, the vulva has more room to open and eggs can be more easily released. The rearward wave of body wall muscle contraction may provide additional peristaltic compression to the uterus and promote egg positioning near the vulva. In an analogous mechanism, a wave of body wall muscle contraction pushes intestinal contents posteriorly just prior to the anal depressor muscle contraction during the defecation motor program (Liu and Thomas, 1994).

Humans and *C. elegans* each have over 70 kinds of K^+ channels that inhibit cell electrical excitability. An overarching issue is to understand for what purpose complex mixtures of K^+ channels that differ in individual cell types limit cell excitability, and how and why neuromodulators then further adjust cell excitability. Our studies have delineated a physiological role for the ERG K^+ channel in limiting excitability of the vulval muscles so that contractions do not occur until an egg-laying active phase is initiated by serotonin. ERG is only one of several K^+ channels known to be expressed in the vulval muscles and/or to affect egg laying. The others include EAG, Kv3/Shaw, and Ca^{2+}-activated K^+ channels (Elkes et al., 1997; Johnstone et al., 1997; Weinshenker et al., 1999; Wang et al., 2001). Gain-of-function mutations in several of these channels inhibit egg laying, but it is less clear if or how loss of these channels affects egg laying. The methods we have developed to successfully delineate how ERG affects egg laying can now be applied to analyzing other K^+ channel mutants and to the many other existing *C. elegans* mutants with decreased or increased egg-laying behavior. Together, this approach should help define at a new level of detail how excitability of the vulval muscles is controlled to generate the two behavioral states of egg laying. In particular, the manner in which serotonin signals through G proteins to increase excitability of the vulval muscles to switch from the inactive to the active phase is open to such analysis.

Supplementary Material

Refer to Web version on PubMed Central for supplementary material.

Acknowledgments

This work was funded by a grant to MRK from the NINDS (NS036918) and by fellowships to KMC from the NIH (GM079813) and the American Heart Association (POST4990016). Confocal instrumentation was supported by a grant to the Yale Liver Center (DK34989). We are grateful to Amy Bany, Andy Bellemer, and Antony Jose for important preliminary work, Rene Garcia, Bob Horvitz, Liqun Luo, Kang Shen, and Paul Sternberg for reagents and discussions, and Sloan Warren, Tony Koleske, and members of the Koelle lab for insightful comments. Some strains used were obtained from the *Caenorhabditis* Genetics Center (CGC).

References

Bany IA, Dong M-Q, Koelle MR. Genetic and cellular basis for acetylcholine inhibition of *Caenorhabditis elegans* egg-laying behavior. J Neurosci. 2003; 23:8060–8069. [PubMed: 12954868]

Bellemer A, Hirata T, Romero MF, Koelle MR. Two types of chloride transporters are required for GABA(A) receptor-mediated inhibition in *C. elegans*. EMBO J. 2011; 30:1852–1863. [PubMed: 21427702]

Brenner S. The genetics of *Caenorhabditis elegans*. Genetics. 1974; 77:71–94. [PubMed: 4366476]

Carnell L, Illi J, Hong SW, McIntire SL. The G-protein-coupled serotonin receptor SER-1 regulates egg laying and male mating behaviors in *Caenorhabditis elegans*. J Neurosci. 2005; 25:10671–10681. [PubMed: 16291940]

Chase DL, Koelle MR. Genetic analysis of RGS protein function in *Caenorhabditis elegans*. Meth Enzymol. 2004; 389:305–320. [PubMed: 15313573]

Clark SG, Lu X, Horvitz HR. The *Caenorhabditis elegans* locus *lin-15*, a negative regulator of a tyrosine kinase signaling pathway, encodes two different proteins. Genetics. 1994; 137:987–997. [PubMed: 7982579]

Dempsey CM, Mackenzie SM, Gargus A, Blanco G, Sze JY. Serotonin (5HT), Fluoxetine, Imipramine and Dopamine Target Distinct 5HT Receptor Signaling to Modulate *Caenorhabditis elegans* Egg-Laying Behavior. Genetics. 2005; 169:1425–1436. [PubMed: 15654117]

Desai C, Garriga G, McIntire SL, Horvitz HR. A genetic pathway for the development of the *Caenorhabditis elegans* HSN motor neurons. Nature. 1988; 336:638–646. [PubMed: 3200316]

Dong MQ, Chase D, Patikoglou GA, Koelle MR. Multiple RGS proteins alter neural G protein signaling to allow *C. elegans* to rapidly change behavior when fed. Genes Dev. 2000; 14:2003–2014. [PubMed: 10950865]

Duerr JS, Gaskin J, Rand JB. Identified neurons in *C. elegans* coexpress vesicular transporters for acetylcholine and monoamines. Am J Physiol, Cell Physiol. 2001; 280:C1616–1622. [PubMed: 11350757]

Edwards SL, Charlie NK, Milfort MC, Brown BS, Gravlin CN, Knecht JE, Miller KG. A novel molecular solution for ultraviolet light detection in *Caenorhabditis elegans*. PLoS Biol. 2008; 6:e198. [PubMed: 18687026]

Elkes DA, Cardozo DL, Madison J, Kaplan JM. EGL-36 Shaw channels regulate *C. elegans* egg-laying muscle activity. Neuron. 1997; 19:165–174. [PubMed: 9247272]

Faumont S, Rondeau G, Thiele TR, Lawton KJ, McCormick KE, Sottile M, Griesbeck O, Heckscher ES, Roberts WM, Doe CQ, Lockery SR. An image-free opto-mechanical system for creating virtual environments and imaging neuronal activity in freely moving *Caenorhabditis elegans*. PLoS ONE. 2011; 6:e24666. [PubMed: 21969859]

Frøkjaer-Jensen C, Davis MW, Hopkins CE, Newman BJ, Thummel JM, Olesen S-P, Grunnet M, Jorgensen EM. Single-copy insertion of transgenes in *Caenorhabditis elegans*. Nat Genet. 2008; 40:1375–1383. [PubMed: 18953339]

Gao S, Zhen M. Action potentials drive body wall muscle contractions in *Caenorhabditis elegans*. Proc Natl Acad Sci USA. 2011; 108:2557–2562. [PubMed: 21248227]

Garcia LR, Sternberg PW. *Caenorhabditis elegans* UNC-103 ERG-like potassium channel regulates contractile behaviors of sex muscles in males before and during mating. J Neurosci. 2003; 23:2696–2705. [PubMed: 12684455]

Hapiak VM, Hobson RJ, Hughes L, Smith K, Harris G, Condon C, Komuniecki P, Komuniecki RW. Dual excitatory and inhibitory serotonergic inputs modulate egg laying in *Caenorhabditis elegans*. Genetics. 2009; 181:153–163. [PubMed: 19001289]

Hardaker LA, Singer E, Kerr R, Zhou G, Schafer WR. Serotonin modulates locomotory behavior and coordinates egg-laying and movement in *Caenorhabditis elegans*. J Neurobiol. 2001; 49:303–313. [PubMed: 11745666]

Hobson RJ, Hapiak VM, Xiao H, Buehrer KL, Komuniecki PR, Komuniecki RW. SER-7, a *Caenorhabditis elegans* 5-HT7-like receptor, is essential for the 5-HT stimulation of pharyngeal pumping and egg laying. Genetics. 2006; 172:159–169. [PubMed: 16204223]

Hu Z, Pym ECG, Babu K, Vashlishan Murray AB, Kaplan JM. A neuropeptide-mediated stretch response links muscle contraction to changes in neurotransmitter release. Neuron. 2011; 71:92–102. [PubMed: 21745640]

Johnstone DB, Wei A, Butler A, Salkoff L, Thomas JH. Behavioral defects in *C. elegans egl-36* mutants result from potassium channels shifted in voltage-dependence of activation. Neuron. 1997; 19:151–164. [PubMed: 9247271]

Jose AM, Bany IA, Chase DL, Koelle MR. A specific subset of transient receptor potential vanilloid-type channel subunits in *Caenorhabditis elegans* endocrine cells function as mixed heteromers to promote neurotransmitter release. Genetics. 2007; 175:93–105. [PubMed: 17057248]

Kim J, Poole DS, Waggoner LE, Kempf A, Ramirez DS, Treschow PA, Schafer WR. Genes affecting the activity of nicotinic receptors involved in *Caenorhabditis elegans* egg-laying behavior. Genetics. 2001; 157:1599–1610. [PubMed: 11290716]

Kuzhikandathil EV, Oxford GS. Dominant-negative mutants identify a role for GIRK channels in D3 dopamine receptor-mediated regulation of spontaneous secretory activity. J Gen Physiol. 2000; 115:697–706. [PubMed: 10828244]

LeBoeuf B, Gruninger TR, Garcia LR. Food deprivation attenuates seizures through CaMKII and EAG K^+ channels. PLoS Genet. 2007; 3:1622–1632. [PubMed: 17941711]

Lee RY, Lobel L, Hengartner M, Horvitz HR, Avery L. Mutations in the alpha1 subunit of an L-type voltage-activated Ca^{2+} channel cause myotonia in *Caenorhabditis elegans*. EMBO J. 1997; 16:6066–6076. [PubMed: 9321386]

Lee T, Luo L. Mosaic analysis with a repressible cell marker for studies of gene function in neuronal morphogenesis. Neuron. 1999; 22:451–461. [PubMed: 10197526]

Li W, Feng Z, Sternberg PW, Xu XZS. A *C. elegans* stretch receptor neuron revealed by a mechanosensitive TRP channel homologue. Nature. 2006; 440:684–687. [PubMed: 16572173]

Liu DW, Thomas JH. Regulation of a periodic motor program in *C. elegans*. J Neurosci. 1994; 14:1953–1962. [PubMed: 8158250]

Liu P, Ge Q, Chen B, Salkoff L, Kotlikoff MI, Wang Z-W. Genetic dissection of ion currents underlying all-or-none action potentials in *C. elegans* body-wall muscle cells. J Physiol (Lond). 2011; 589:101–117. [PubMed: 21059759]

Lüscher C, Nicoll RA, Malenka RC, Muller D. Synaptic plasticity and dynamic modulation of the postsynaptic membrane. Nature Neuroscience. 2000; 3:545–550.

Marder E, Bucher D. Understanding circuit dynamics using the stomatogastric nervous system of lobsters and crabs. Annu Rev Physiol. 2007; 69:291–316. [PubMed: 17009928]

McDonald TF, Pelzer S, Trautwein W, Pelzer DJ. Regulation and modulation of calcium channels in cardiac, skeletal, and smooth muscle cells. Physiol Rev. 1994; 74:365–507. [PubMed: 8171118]

McNally K, Audhya A, Oegema K, McNally FJ. Katanin controls mitotic and meiotic spindle length. J Cell Biol. 2006; 175:881–891. [PubMed: 17178907]

Mello C, Fire A. DNA transformation. Methods Cell Biol. 1995; 48:451–482. [PubMed: 8531738]

Moresco JJ, Koelle MR. Activation of EGL-47, a Galpha(o)-coupled receptor, inhibits function of hermaphrodite-specific motor neurons to regulate *Caenorhabditis elegans* egg-laying behavior. J Neurosci. 2004; 24:8522–8530. [PubMed: 15456826]

Petersen CI, McFarland TR, Stepanovic SZ, Yang P, Reiner DJ, Hayashi K, George AL, Roden DM, Thomas JH, Balser JR. In vivo identification of genes that modify ether-a-go-go-related gene activity in *Caenorhabditis elegans* may also affect human cardiac arrhythmia. Proc Natl Acad Sci USA. 2004; 101:11773–11778. [PubMed: 15280551]

Reiner DJ, Weinshenker D, Tian H, Thomas JH, Nishiwaki K, Miwa J, Gruninger T, Leboeuf B, Garcia LR. Behavioral genetics of *Caenorhabditis elegans unc-103*-encoded erg-like K(+) channel. J Neurogenet. 2006; 20:41–66. [PubMed: 16807195]

Ringstad N, Horvitz HR. FMRFamide neuropeptides and acetylcholine synergistically inhibit egg-laying by *C. elegans*. Nat Neurosci. 2008; 11:1168–1176. [PubMed: 18806786]

Sanguinetti MC, Tristani-Firouzi M. hERG potassium channels and cardiac arrhythmia. Nature. 2006; 440:463–469. [PubMed: 16554806]

Shyn SI, Kerr R, Schafer WR. Serotonin and Go modulate functional states of neurons and muscles controlling *C. elegans* egg-laying behavior. Curr Biol. 2003; 13:1910–1915. [PubMed: 14588249]

Spilker KA, Wang GJ, Tugizova MS, Shen K. *C. elegans* Muscleblind homolog mbl-1 functions in neurons to regulate synapse formation. Neural Development. 2012; 7:7. [PubMed: 22314215]

Tanis JE, Bellemer A, Moresco JJ, Forbush B, Koelle MR. The potassium chloride cotransporter KCC-2 coordinates development of inhibitory neurotransmission and synapse structure in *Caenorhabditis elegans*. J Neurosci. 2009; 29:9943–9954. [PubMed: 19675228]

Tanis JE, Moresco JJ, Lindquist RA, Koelle MR. Regulation of serotonin biosynthesis by the G proteins Galphao and Galphaq controls serotonin signaling in *Caenorhabditis elegans*. Genetics. 2008; 178:157–169. [PubMed: 18202365]

Tian L, Hires SA, Mao T, Huber D, Chiappe ME, Chalasani SH, Petreanu L, Akerboom J, McKinney SA, Schreiter ER, Bargmann CI, Jayaraman V, Svoboda K, Looger LL. Imaging neural activity in worms, flies and mice with improved GCaMP calcium indicators. Nat Methods. 2009; 6:875–881. [PubMed: 19898485]

Waggoner LE, Dickinson KA, Poole DS, Tabuse Y, Miwa J, Schafer WR. Long-term nicotine adaptation in *Caenorhabditis elegans* involves PKC-dependent changes in nicotinic receptor abundance. J Neurosci. 2000; 20:8802–8811. [PubMed: 11102488]

Waggoner LE, Zhou GT, Schafer RW, Schafer WR. Control of alternative behavioral states by serotonin in *Caenorhabditis elegans*. Neuron. 1998; 21:203–214. [PubMed: 9697864]

Wang ZW, Saifee O, Nonet ML, Salkoff L. SLO-1 potassium channels control quantal content of neurotransmitter release at the *C. elegans* neuromuscular junction. Neuron. 2001; 32:867–881. [PubMed: 11738032]

Weinshenker D, Garriga G, Thomas JH. Genetic and pharmacological analysis of neurotransmitters controlling egg laying in *C. elegans*. J Neurosci. 1995; 15:6975–6985. [PubMed: 7472454]

Weinshenker D, Wei A, Salkoff L, Thomas JH. Block of an ether-a-go-go-like K(+) channel by imipramine rescues *egl-2* excitation defects in *Caenorhabditis elegans*. J Neurosci. 1999; 19:9831–9840. [PubMed: 10559392]

White JG, Southgate E, Thomson JN, Brenner S. The structure of the nervous system of the nematode *Caenorhabditis elegans*. Phil Trans Royal Soc. 1986; 314:1–340.

Zhang M, Chung SH, Fang-Yen C, Craig C, Kerr RA, Suzuki H, Samuel ADT, Mazur E, Schafer WR. A self-regulating feed-forward circuit controlling *C. elegans* egg-laying behavior. Curr Biol. 2008; 18:1445–1455. [PubMed: 18818084]

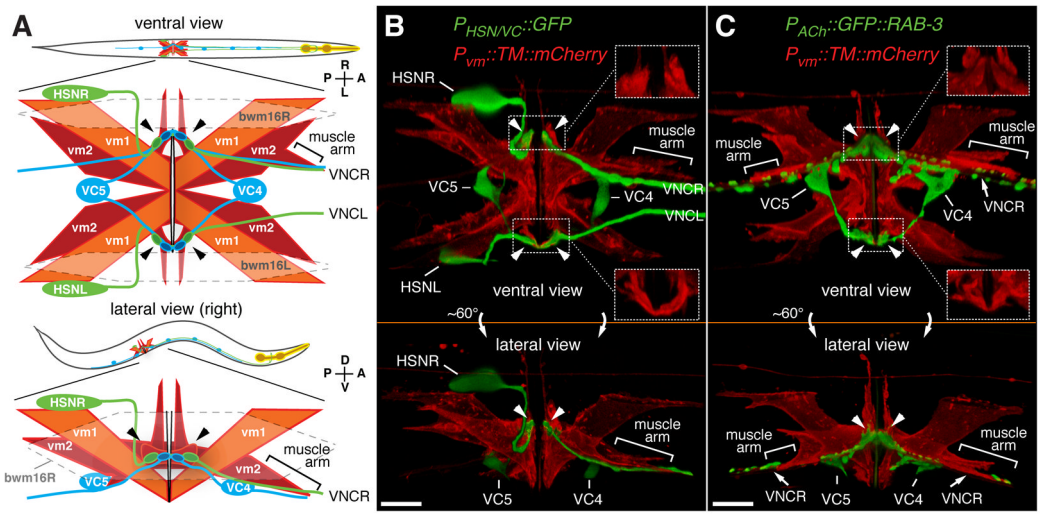

Figure 1. Anatomy of the egg-laying system

(A) Cartoons showing ventral (top) or lateral (bottom) views of *C. elegans* and expanded views of the egg-laying system. HSN (green) and VC (blue) motor neurons as well as vm1 (orange) and vm2 (red) vulval muscles are shown. Six VC neurons send processes along the right ventral nerve cord (VNC). VC4 and VC5 have cell bodies close to the vulva and extend processes bilaterally to the vm2s. vm2 cells extend arms laterally onto which HSN and VC presynaptic termini form (arrowheads). vm2 cells on the right side also extend separate muscle arms (brackets) which receive additional synapses from the right ventral nerve cord. Gap junctions electrically connect vm cells, but anterior and posterior vm cells appear to be isolated from each other (solid black lines) but postsynaptic to the same neurons. The vulval muscles fill a gap between body wall muscle cells bwm16L/R (indicated with dashed line). Axes indicating Anterior, Posterior, Left, Right, Dorsal, and Ventral are shown here and in subsequent figures. Micrographs and schematics in this work are often right lateral views to allow visualization of the synapses between vm2 and the right ventral nerve cord.

(B) Presynaptic motor neurons interact with the vulval muscle at a large postsynaptic terminus. Transgenic worms expressed mCherry fused to a transmembrane domain (TM::mCherry) at the plasma membrane from a vulval-muscle specific promoter (P_{vm}) and expressed GFP from a second promoter strongly in the HSN and weakly in the VC4 and VC5 neurons. Arrowheads indicate presynaptic varicosities, and regions indicated with dotted boxes are magnified at right corners (150%) with only TM::mCherry labeling to reveal the vulval muscle postsynaptic termini onto which the HSN and VCs make synaptic contact. Bar, 10 μm.

(C) Same as (B) except that the GFP label is the presynaptic marker GFP::RAB-3 expressed in all cholinergic neurons. This marker fills out the VC4 and VC5 cell bodies and labels their presynaptic termini onto the vm2 lateral projections (arrowheads). It also produces punctate labeling of additional ventral nerve cord (VNC) synapses, and these may include the synapses made between VC neurons, by VCs onto vm2 muscle arms (brackets), and by other ventral nerve cord motor neurons onto vm1 cells (White, J.G. et al., 1986). Bar, 10 μm.

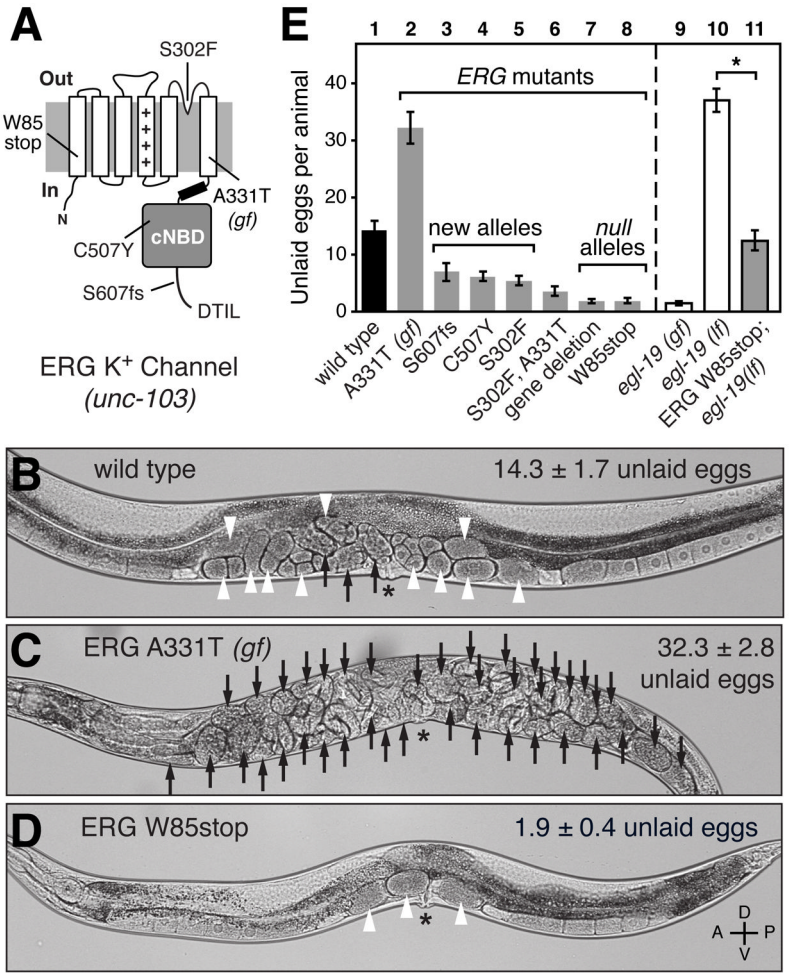

Figure 2. The ERG K^+ channel inhibits *C. elegans* egg-laying behavior

(A) Cartoon of the *C. elegans* ERG K^+ channel and location of mutations. ++++, voltage-sensor; cNBD, cyclic nucleotide binding domain; fs, predicted frameshift mutation; gf, gain-of-function mutation; DTIL, predicted carboxy-terminal PDZ interaction motif. The W85stop mutant is used as the standard ERG null background in this work.

(B–D) Brightfield micrographs of wild-type *C. elegans* (B), the A331T ERG gain-of-function mutant (C), or the W85stop ERG null mutant (D). Black arrows indicate eggs with more than 8 cells, and white arrowheads indicate early-stage eggs of 8 cells or fewer. The average number of unlaid eggs per animal (n=30) is indicated ±95% confidence intervals. The A331T gain-of-function mutant accumulates unlaid eggs because it rarely lays them, while the ERG null mutant retains only ~two of the most recently produced eggs since it lays eggs too frequently. Asterisk, vulva; worm anterior is on left.

(E) Quantification of unlaid eggs in animals bearing ERG K^+ channel and L-type Ca^{2+} channel mutations. Wild-type animals (bar 1) were compared to the ERG A331T gain-of-function mutant (bar 2) and ERG loss-of-function mutants (bars 3–8). Gain- *(gf)* and loss of function *(lf)* mutations in *egl-19,* which encodes the sole α_1 subunit of the *C. elegans* L-type Ca^{2+} channel, were tested individually or in combination with an ERG null mutation. Error bars here and in all subsequent figures represent 95% confidence intervals. Asterisk, $p<0.0001$ (t-test); n=30 animals per genotype.

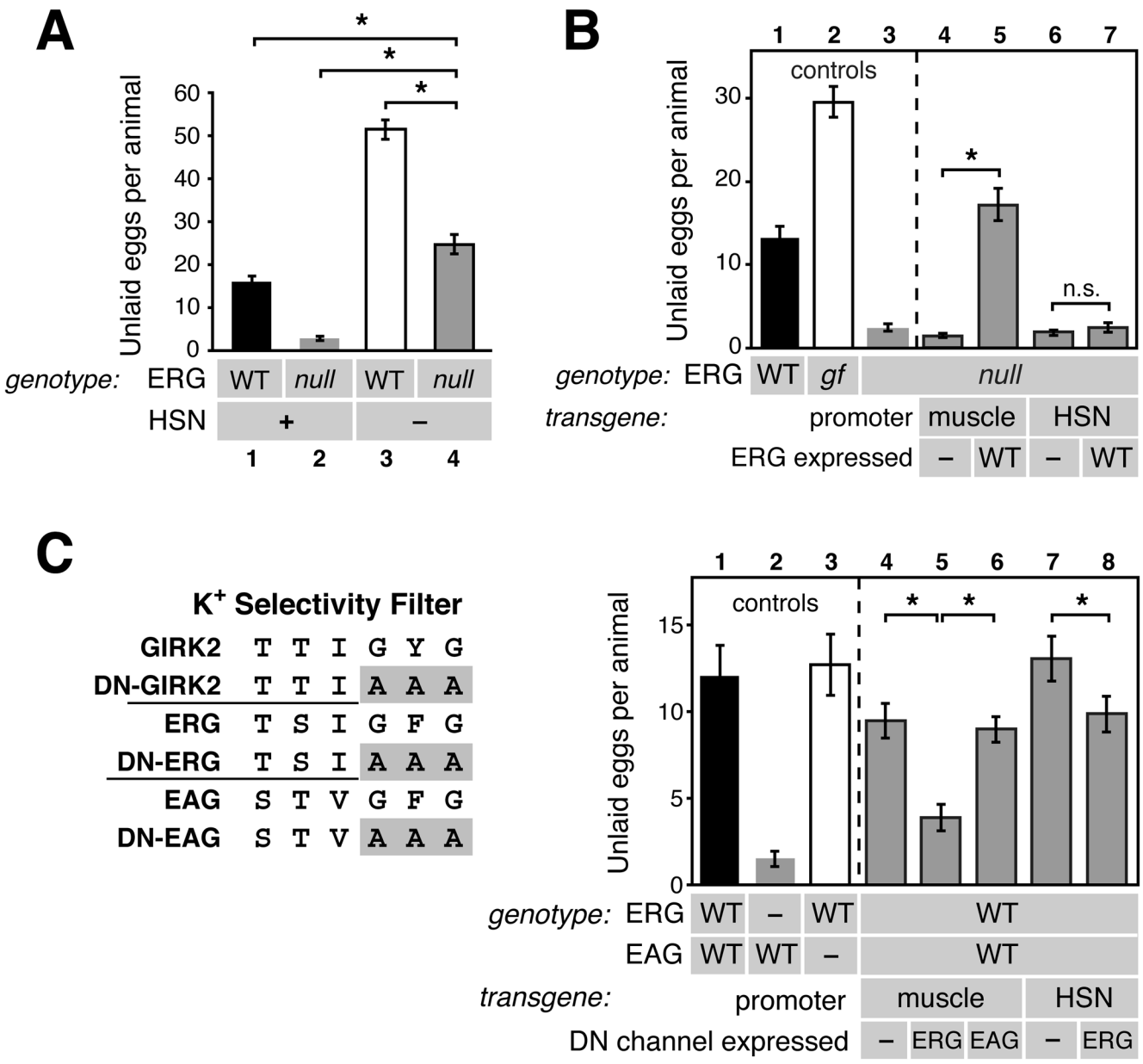

Figure 3. ERG acts in vulval muscles to inhibit egg-laying behavior

(A) ERG acts outside the HSNs, but HSNs are required for the hyperactive egg-laying behavior of ERG null mutants. The number of unlaid eggs that accumulate in the wild type (bar 1), W85stop ERG null mutants (2), *egl-1(dm)* mutants that lack the HSNs (3), and ERG null*; egl-1(dm)* double mutant animals (4) were compared (asterisks, $p<0.0001$ (one-way ANOVA); n=30 animals).

(B) Expression of ERG in muscle is sufficient to inhibit egg-laying behavior. Unlaid eggs were counted in the wild type (bar 1), the A331T ERG gain-of-function mutant (*gf*, bar 2), the W85stop ERG null mutant (bar 3), or in null mutant animals bearing various transgenes. The *myo-3* promoter was used to drive muscle expression of either no channel (−, bar 4) or wild-type ERG (WT, bar 5) in the vulval muscles. The *tph-1* promoter was used to drive HSN expression of either no channel (−, bar 6) or wild-type ERG (WT, bar 7). For (A) and

(B), asterisks, $p<0.0003$ (t-test); n=30 for non-transgenic animals and n=50 for transgenic animals (10 from each of five lines per transgene); *n.s.* (not significant) indicates $p>0.05$. (C) ERG in muscle is necessary for inhibition of egg-laying behavior. Based on a previous dominant-negative (DN) GIRK2 channel mutant (Kuzhikandathil and Oxford, 2000), the GFG residues in the K^+ channel selectivity filter were mutated to AAA to generate dominant-negative (DN) ERG and EAG mutants. Unlaid eggs were counted in the wild type (bar 1), an ERG null mutant (bar 2), an EAG null mutant (bar 3), or in wild-type animals bearing transgenes expressing nothing (−), DN-ERG, or DN-EAG in either the muscles (bars 4–6) or HSN (bars 7–8).

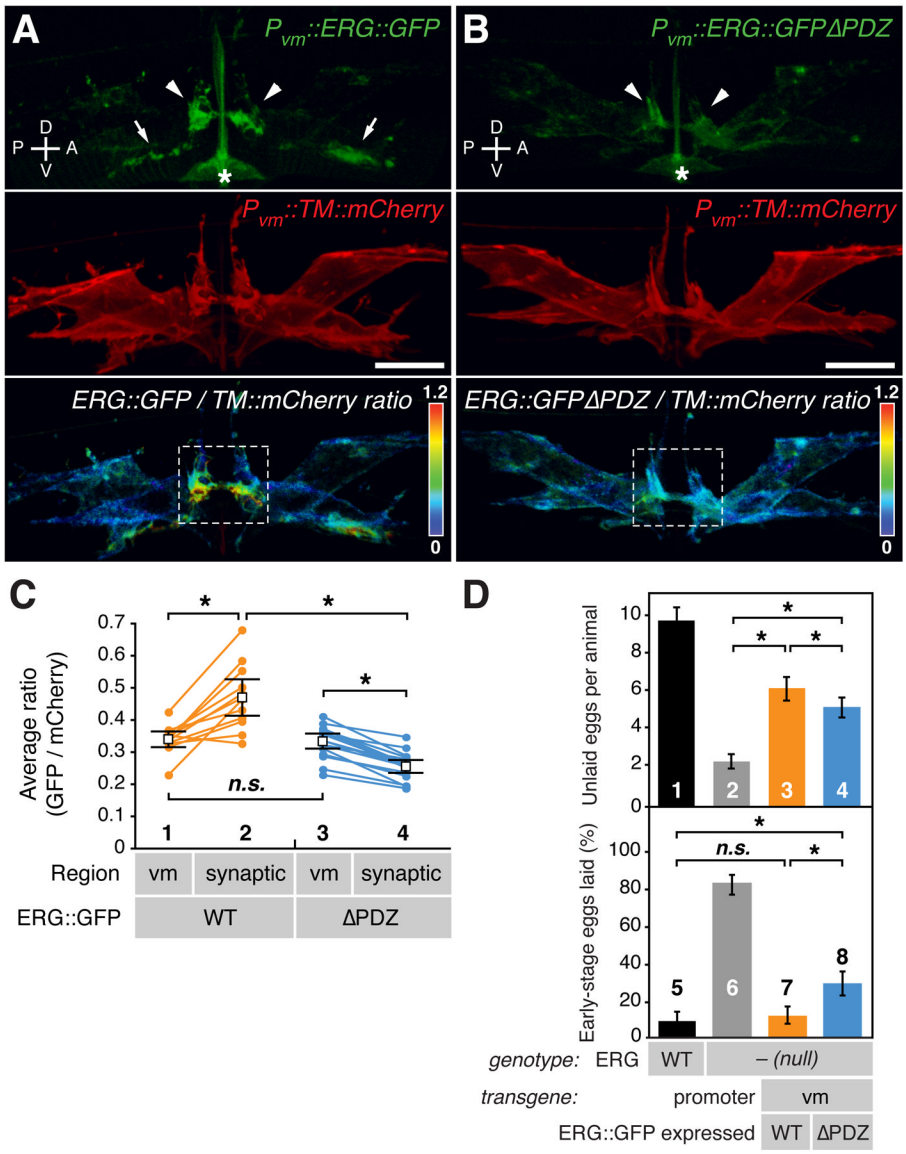

Figure 4. ERG is localized in vulval muscle to the postsynaptic termini via a PDZ interaction motif

(A and B) Representative ratiometric images of ERG localization. (A) ERG bearing internally-inserted GFP (ERG::GFP) was expressed in vulval muscle from the *unc-103e* promoter (P_{vm}). Its localization (top) was compared to that of a co-expressed transmembrane control protein (TM::mCherry, middle) using ratiometric imaging (bottom). (B) An ERG mutant lacking the putative PDZ-interaction motif (-DTIL) at its carboxy-terminus (ERG::GFPΔPDZ) is shown as in (A). ERG::GFP was enriched at lateral postsynaptic sites (arrowheads) and along the ventral cord (arrows). Dashed white boxes indicate regions of lateral vm2 processes selected for quantitation in (C). Asterisks, the autofluorescent vulval slit; bar, 10 μm; rainbow scale, GFP/mCherry ratio.

(C) Statistical analysis of ratiometric imaging. ERG::GFP to TM::mCherry ratios for entire set of vulval muscles (vm) on one side of a animal are compared to the ratio within the lateral synaptic subregion (white boxes in A and B). Paired measurements from the same

animal are connected by lines; n=12 for wild-type ERG and n=17 for the ΔPDZ mutant. Average ratio pairs are shown; asterisks, $p<0.0004$ (t-test); n.s., not significant with $p>0.05$. (D) Postsynaptic enrichment of ERG is required for proper inhibition of egg laying. Wild-type (bars 1) or the W85stop ERG mull mutants (bars 2–4) bearing transgenes expressing either wild-type ERG::GFP (bars 3) or the ERG::GFPΔPDZ mutant (bars 4) from the vm-specific promoter were assayed for egg-laying behavior. *(top)* Unlaid eggs per animal; asterisks, $p<0.0001$ (*t*-test; n=60 animals per genotype). *(bottom)* Percent of eggs laid at early stages (8 cells or fewer); asterisks, $p<0.0001$; n.s., not significant with $p>0.05$ (Fisher's exact test; n >195 eggs per genotype).

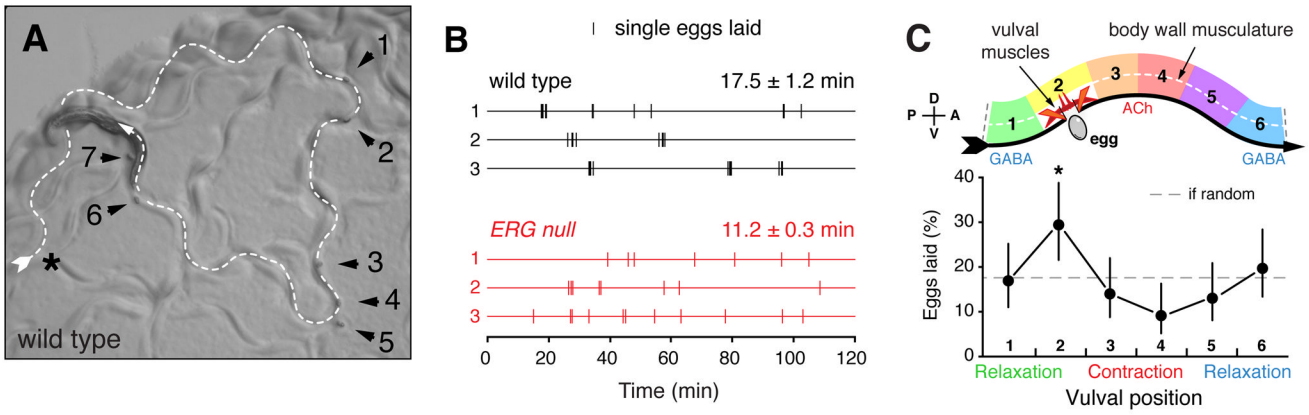

Figure 5. Egg laying occurs in active phases, is rhythmically phased with the body bends of locomotion, and occurs at shorter intervals in ERG null mutants

(A) Eggs are laid during brief active phases. Micrograph of a wild-type worm on a standard NGM agar plate with a lawn of bacterial food during the active phase of egg laying. Worm anterior is to the left, the dashed arrow indicates the track of worm locomotion, and arrowheads show seven eggs laid during one active phase.

(B) Egg laying on standard NGM agar plates with food was followed by video recording for two hours in each of six wild-type and six ERG null (W85stop) mutant animals. Videos were reviewed to identify the specific time points when each egg was laid (vertical hash marks), and representative data from three wild-type animals (black) and three ERG null mutant animals (red) are shown (lines 1–3). The wild type typically lays multiple eggs during a <4 minute active phase followed by a longer interval with no egg laying. ERG null mutants typically lay only a single egg per active phase, likely because they contain only ~two eggs in their uterus, of which only one may be in position to be laid. We determined the inter-cluster time constant from the slope of the log-tail distribution of inter-cluster intervals (> 4 min), as previously described (Waggoner et al., 1998). The deduced intervals are shown ± SEM and significantly different (p<0.0001, analysis of covariance).

(C) Egg laying is phased with the sinusoidal body bends that drive locomotion. Cartoon (top) of the vulval muscles and ventral body wall muscles (dashed lines) during one sinusoidal wavelength of locomotion as the animal moves to its anterior on right (ventral arrow). This idealized wave was segmented into six regions (1–6). (bottom) From video recordings from each of six wild-type animals (two hours each), the vulval position during 104 egg laying events was determined. The proportion of eggs laid at each body bend region is shown; asterisks, p=0.0058 (region 2), p=0.039 (region 4, Fisher's exact test).

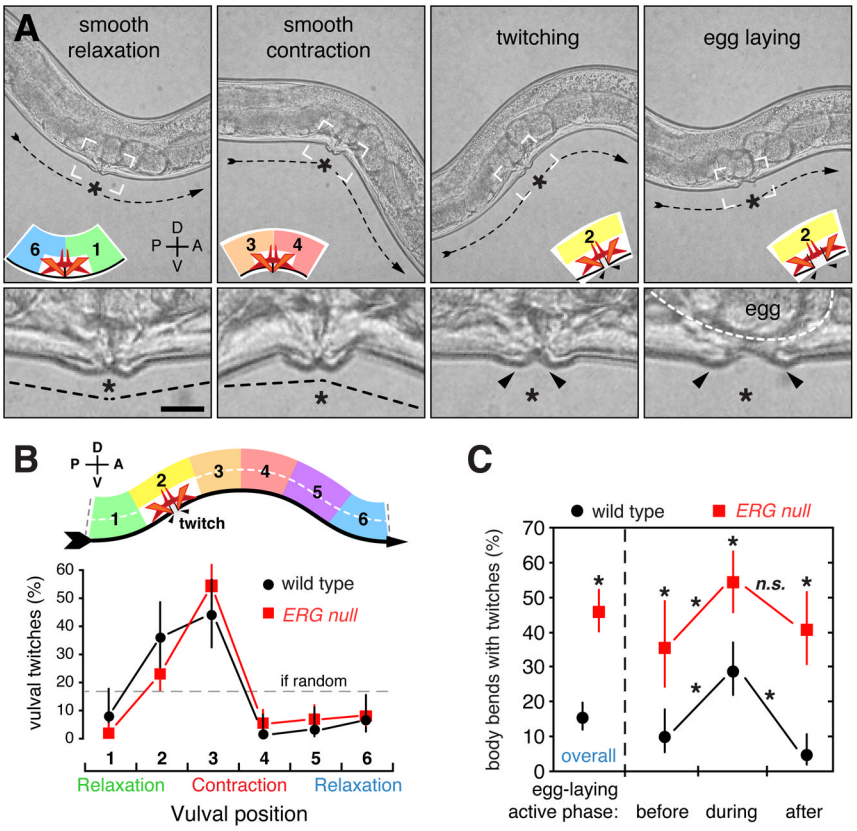

Figure 6. Vulval muscle contractions are phased with respect to locomotor body bends and are limited by ERG

(A) High-speed video recordings of freely behaving worms reveal four vulval muscle excitability states: smooth relaxation, smooth contraction, twitching, and egg laying. (top) Still frames are shown from an ERG null mutant recording where the twitches are more easily seen compared to wild type animals (Movie 1). Dashed arrows indicate worm direction and posture. Smooth relaxation occurs when the vulva passes through the ventral relaxation trough while smooth contraction occurs at the ventral contraction crest. Twitches are visible vulval muscle contractions that move and separate the tips of the vulva, while egg laying accompanies full vulval opening and egg release. Inset cartoons indicate position of the vulva within the idealized wave, and white boxes indicate regions of high magnification insets (bottom). Asterisk, vulva; arrowheads, opening of the vulva during twitching and egg laying. Scale bar, 10 μm.

(B) Vulval muscle twitching is phased with locomotion. High-speed video was used to record the timing of twitches in five wild-type and five ERG null mutant animals. Each video included 5 minutes prior to and 7 minutes after the first egg-laying event. Twitches were mapped relative to the timing of vulval muscle smooth contractions and relaxations (top) as it moves to its anterior on right (ventral arrow). Points indicate the proportion of twitches that occurred at each position; wild type: black circles, n=61 twitches; ERG null mutants: red squares, n=160 twitches.

(C) Vulval muscle twitching increases during egg laying and is more frequent in ERG null mutants. From the high-speed data in B, the frequency of body bends with twitches was determined. One minute prior to and three minutes after the first egg laying event was designated as the active phase for paired analyses; asterisks, $p<0.0001$ (Fisher's exact test); n.s., not significant ($p>0.05$).

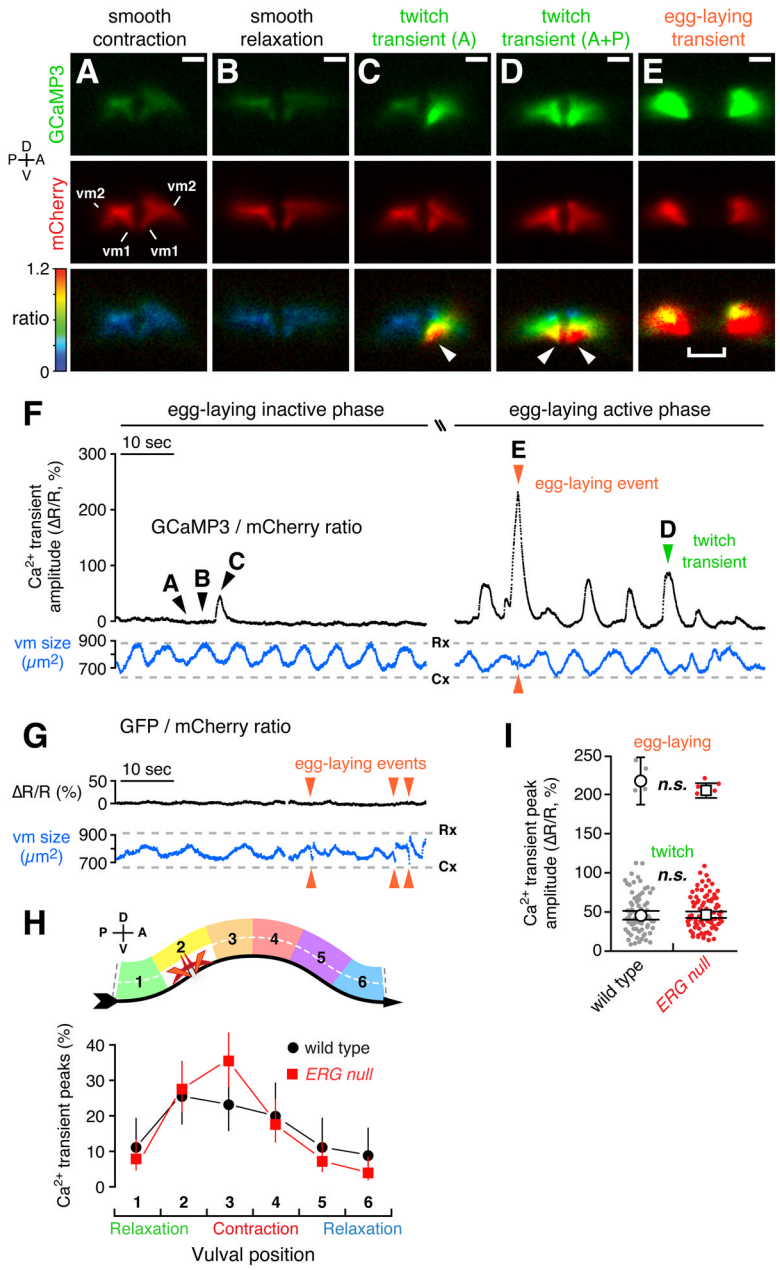

Figure 7. Distinct vulval muscle Ca^{2+} transients mediate twitching and egg-laying behaviors

(A–E) Ratiometric Ca^{2+} imaging in the vulval muscles in behaving animals. Three 1-minute recordings were made for each of ten wild type and ten ERG null animals. GCaMP3 (top) and mCherry (middle) fluorescence, and the GCaMP3/mCherry intensity-modulated ratio (bottom) images from a wild-type animal are shown and correspond to the time points indicated by arrowheads labeled A–E in panel (F). (C) A twitch transient in the anterior half of the vulva. (D) A twitch transient occurring in both anterior and posterior halves. Arrowheads, subcellular localization of the GCaMP3/mCherry ratio peak at the vulval tips. Separation of the two halves of the vulva in (E) is due to contraction of the vulval muscles and the passage of an egg through the vulva. Bar, 10 μm; positions of vm1 and vm2 are indicated. See also Movies 2 and 3.

(F) Traces from a representative wild-type animal are shown of the average GCaMP3/mCherry ratio in the vulval muscles (ΔR/R, black trace) prior to (left side; Movie 2) and during the egg-laying active phase (right side; Movie 3). Traces of the area of the mCherry signal (blue) indicate changes in vulval muscle (vm) size during locomotion (Cx, smooth contraction; Rx, smooth relaxation). Arrowheads indicate Ca^{2+} transients that mediate egg-laying and twitching contractions.
(G) Ratiometric imaging in the vulval muscles in behaving animals expressing the Ca^{2+} insensitive GFP along with mCherry. Egg-laying contractions (arrowheads) appear as events in the vulval muscle size trace (blue) but are silent in the GFP/mCherry ratio.
(H) Vulval muscle Ca^{2+} transients are phased with locomotion. Six-minute recordings were made for each of six wild-type and ERG null animals. The peak of each Ca^{2+} transient was mapped relative to the timing of vulval muscle smooth contractions and relaxations (top) as the animal moves to its anterior on right (ventral arrow). Points indicate the proportion of transients that occurred at each position; wild type: black circles, n=90 transients; ERG null mutants: red squares, n=152 transients).
(I) Peak GCaMP3/mCherry ratio (ΔR/R) amplitudes for Ca^{2+} transients recorded from three one-minute recordings from each of ten wild type and ten ERG null animals are shown in a scatter plot (grey, n=85 wild type transients; red, n=102 ERG null mutant transients, red). Transients were grouped by peak ΔR/R amplitude into egg laying (>120%) and twitch (0–120%) transients. Open circles (wild type) and squares (ERG null) indicate the mean amplitude for each group; n.s., not significant (p>0.05; t-test).

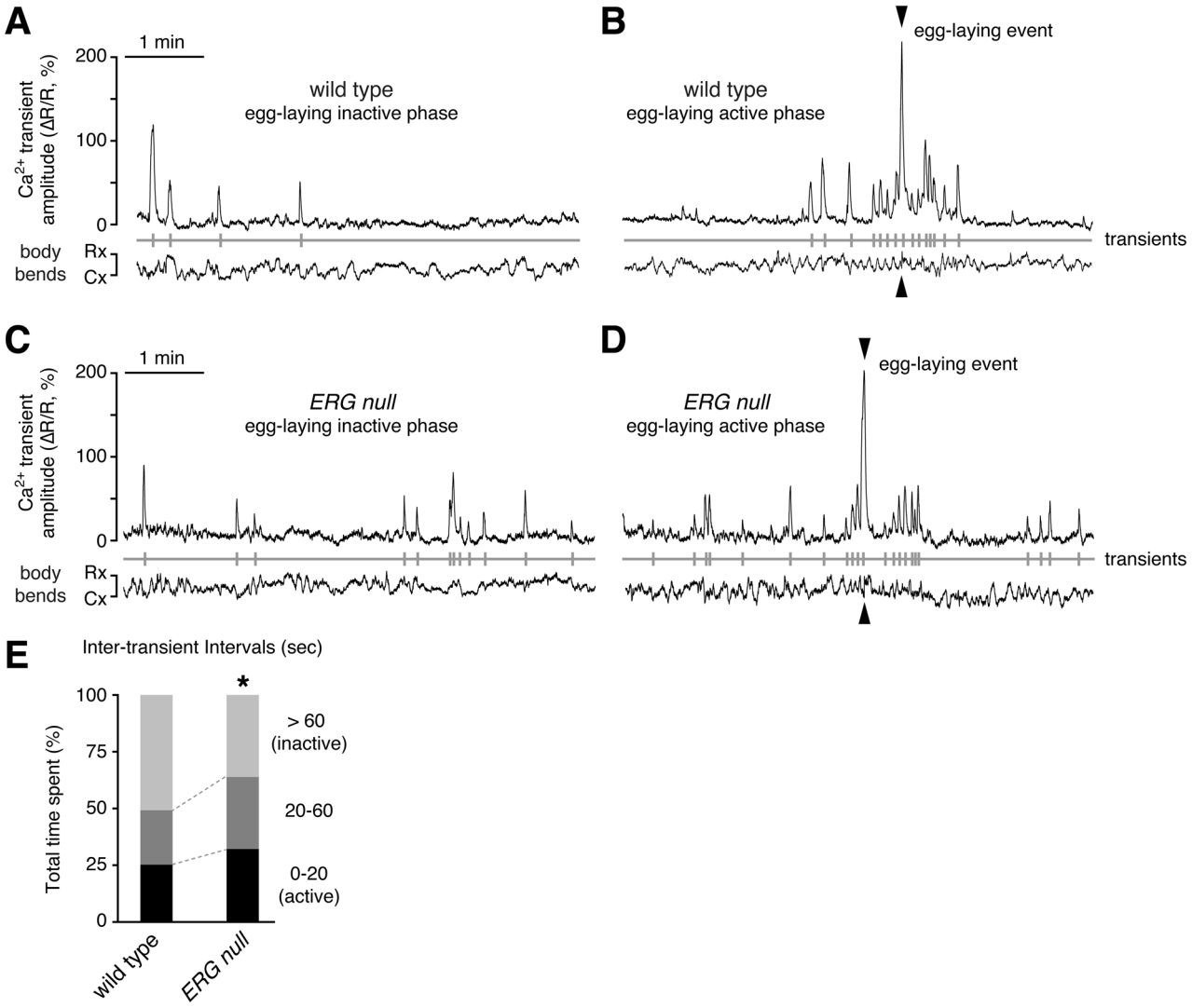

Figure 8. Increased frequency of rhythmic Ca^{2+} transients in ERG null mutants

(A–D) Ratiometric Ca^{2+} imaging in the vulval muscles in behaving animals. Six-minute recordings were made for each of twelve wild-type and ERG null mutant animals. Representative traces shown indicate the average GCaMP3/mCherry ratio (ΔR/R) in the vulval muscles of separate wild-type (A and B) and ERG null mutant animals (C and D) during an egg-laying inactive phase (A and C) or the egg-laying active phase (B and D). Transients with peak magnitude ≥20% ΔR/R (vertical grey lines) were used to define inter-transient intervals (below). Traces of the area of the mCherry signal indicate changes in vulval muscle size during body bends (Cx, smooth contraction; Rx, smooth relaxation). (E) Egg-laying muscles of ERG null mutants have more frequent Ca^{2+} transients. Transients with ΔR/R ≥20% were used to define inter-transient intervals from twelve wild type and twelve ERG null mutant animals. Intervals (wild type, n=201; ERG null, n= 240) were grouped by their duration (0–20 sec, 20–60 sec, and >60 sec), and the total time spent within each group is shown as a percent of total recording time (~72 min per genotype). Asterisk, $p<0.0001$ (chi-square test).

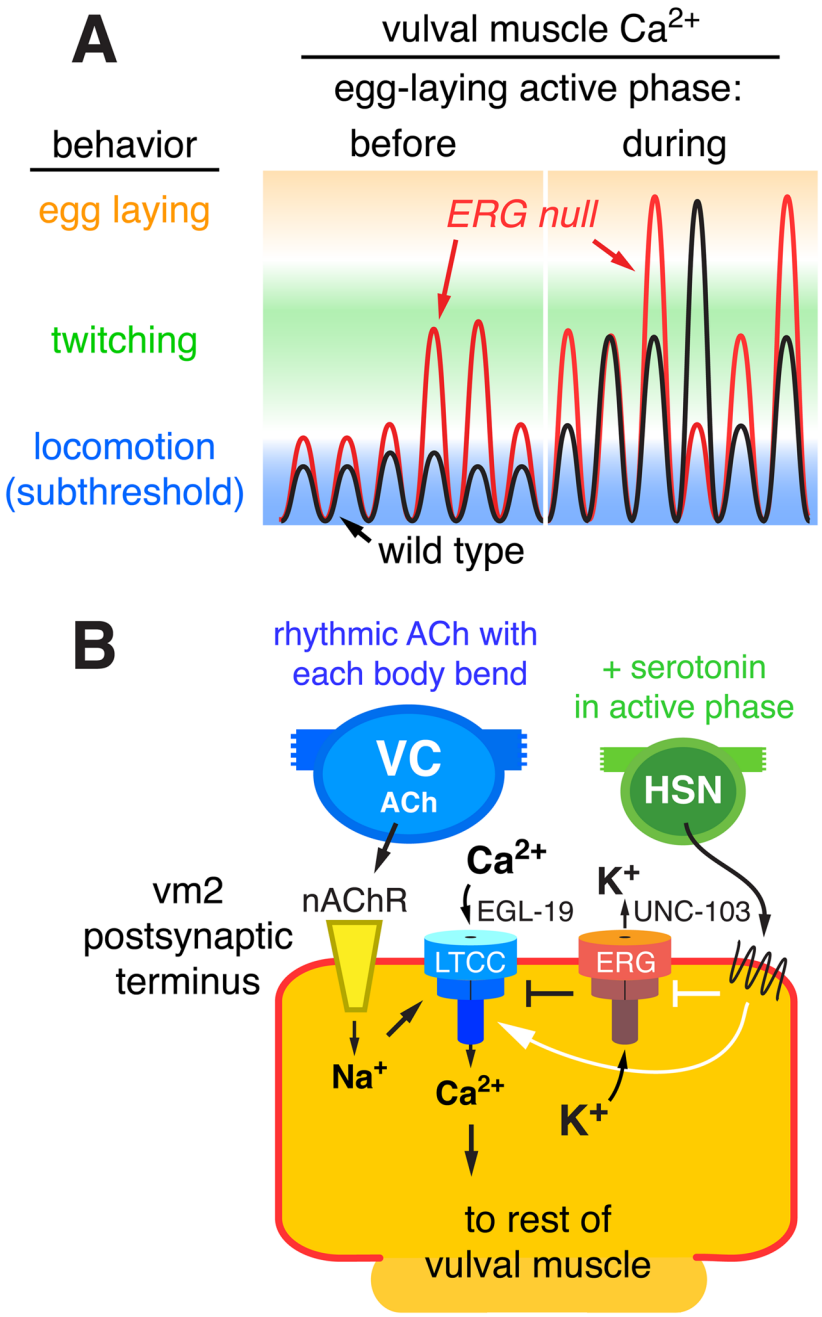

Figure 9. Working model: ERG limits postsynaptic Ca^{2+} transients and behavioral responses to rhythmic synaptic excitation

(A) Schematic of vulval muscle Ca^{2+} signals on a log scale during six body bends before and six more body bends during the active phase of egg laying. Before the active phase, excitatory postsynaptic potentials are subthreshold and do not trigger detectable vulval muscle Ca^{2+} transients or contraction. During the active phase, increased postsynaptic electrical excitability increases the probability of Ca^{2+} transients that drive vulval muscle twitching (green) or large transients that drive complete vulval muscle contraction and egg laying (orange). In the ERG null mutant (red trace), elevated postsynaptic excitability during

both the inactive and active phases increases the probability of super-threshold responses that trigger Ca^{2+} transients.

(B) Schematic of control of synaptic excitation at the vulval muscles. ACh release from the VC motor neurons, occurring rhythmically at a particular phase of each locomotor body bend, activates nAChR on the vm2 postsynaptic terminus. The resulting local membrane depolarization from Na^{+} influx activates EGL-19 voltage-gated L-type Ca^{2+} channels (LTCC) and plasma membrane Ca^{2+} entry. UNC-103 ERG K^{+} channels localize to and promote repolarization of the postsynaptic terminus to antagonize LTCC activity and keep postsynaptic Ca^{2+} levels at a subthreshold level that fails to trigger vulval muscle contraction. Loss of ERG leads to sustained Ca^{2+} entry through LTCC. The HSN motor neuron releases serotonin that acts through G protein coupled receptors to increase vulval muscle response to ACh and promote the active phase of egg-laying behavior. Solid white arrows and bar indicate possible targets of serotonin signaling: activation of Ca^{2+} signaling through LTCC and/or inhibition of ERG.